Electric control of the Josephson current-phase relation in a topological circuit

J. Wang, L. Hao, and Jun-Feng Liu*
Department of Physics, Southeast University, Nanjing 210096, China
and Department of Physics, South University of Science and Technology of China, Shenzhen 518055, China
(Received 1 December 2015; revised manuscript received 4 February 2016; published 5 April 2016)

We study the current-phase relation of a topological ring-shape Josephson junction, where the ring structure is defined by one-dimensional topological interface states constructed in a two-dimensional honeycomb-lattice system. We show that control of the potential difference between the two ring arms can lead to a φ_0 Josephson junction. The physics origin is the superconducting electron- and holelike quasiparticles possessing a valley-dependent chirality and moving separately in the two ring arms. Our findings provide a purely electric way to consecutively manipulate the Josephson current-phase relation.

DOI: 10.1103/PhysRevB.93.155405

I. INTRODUCTION

For the past decades, Josephson junctions (JJs) have been attracting much attention of researchers, both from a fundamental physics point of view and from the potential applications [1]. For example, the π state JJ has been proposed as circuit elements for quantum computation [2,3] and as on-chip π phase shifters or π batteries for various self-biasing quantum and classical circuits [4–6]. Usually, an s-wave superconductor (S) weak link exhibits a sinusoidal current-phase relation, $J = J_0 \sin\varphi$, where φ is the macroscopic phase difference between the two S banks. As the quasiparticles transport in an exchange-field environment such as in the S/F/S junction (F, ferromagnetic metal) [7–10], the JJ ground state may be at $\varphi = \pi$, referred to as the π-state junction, so the current-phase relation (CPR) has $J = J_0 \sin(\varphi + \pi)$. This crucially depends on the exchange-field strength and environmental temperature. When there are additional spin-nonlinear interactions like the spin-orbit coupling in the system [11–17], the JJ ground state may be at a nonzero phase φ_0, called the φ_0 junction with $J = J_0 \sin(\varphi + \varphi_0)$. Certainly, an external magnetic field can easily implement a φ_0 junction or together with other system parameters [18,19]. The φ-JJ was also proposed and experimentally confirmed by integrating the 0-state and π-state JJs together into a parallel circuit [20–26]; its ground state could be at an arbitrary phase $\pm\varphi$, behind which the second harmonic term of supercurrent plays a dominative role in the current-phase relation.

So far, the CPR modulation for either forming a π state or φ_0-JJ depends heavily on a nonzero exchange field or magnetic field. How to obtain an controllable φ_0 JJ without using magnetization or how to consecutively and electrically change φ_0 in a single JJ is still a challenge even on the theoretical side. The mechanism of the π state in the S/F/S junction [9] is that the spin-opposite quasiparticles accumulate an opposite dynamic phase difference (φ_0) due to the spin splitting in the F layer. This reminds us that a φ_0-JJ might be generated if the Fermi (spin) doubling of the link was removed like in a chiral metal [27,28], while this φ_0 might be modulated by a static potential difference, if the electronlike and holelike quasiparticles were separated spatially.

Following the above route, we propose in this work an electrically controllable φ_0-JJ, which is based on the valley-helical interfacial (or *inner boundary*) state [29–33] of a quantum valley Hall insulator [34] forming in two-dimensional (2D) buckled honeycomb-lattice systems. This topological interface state (TIS), consisting of two valley-opposite chiral states, can be split in real space by photoirradiation [35]. The splitting TIS together with the two S leads are devised into a ringlike JJ. Based on this model, we will show that a potential difference applied on one of the ring arms can lead to a controllable φ_0-JJ.

Our paper is organized in the following manner. In Sec. II, we describe the model Hamiltonian of the ring-shape JJ and present numerical calculations of supercurrent. The Andreev bound states are also computed to explain the anomalous Josephson effect. In Secs. III and IV, the two independent lattice models are studied to further support the obtained results in Sec. II. A continuum model is also given in Sec. V. Our conclusions are summarized in the last section.

II. φ_0-JJ BASED ON VALLEY-CHIRAL TIS

Let us start from the TISs constructed in the 2D buckled honeycomb-lattice materials such as silicene [36,37], germanene [38,39], stanene [40], as well as some manganese chalcogenophosphates [41] ($MnPX_3$, $X = S$, Se). A few topological phases were found in those materials, and the TISs were demonstrated to be readily built by using a perpendicular field E_z [29–33]. On the other hand, besides the spin degree of freedom, an extra valley degree of freedom of Dirac electrons arises and is helpful to split superconducting Cooper pairs spatially [42,43] in a superconductor device. We first consider the valley-chiral TISs generated in a finite-size nanoribbon model in Fig. 1(a), which is described by

$$\mathcal{H} = -t\sum_{\langle ij\rangle\sigma} C^\dagger_{i\sigma}C_{j\sigma} + \sum_{i\sigma}(\mu_i E_z + V_g)C^\dagger_{i\sigma}C_{i\sigma} + i\sum_{\langle\langle lm\sigma\rangle\rangle}\frac{\Omega\nu_{lm}}{3\sqrt{3}}C^\dagger_{l\sigma}C_{m\sigma}, \quad (1)$$

where the first term is the nearest-neighbor hopping with strength t, E_z in a unit of energy denotes the staggered potential, and V_g denotes the possible gate voltage applied in certain lattice sites. The third term is the Haldane interaction

*liujf@sustc.edu.cn

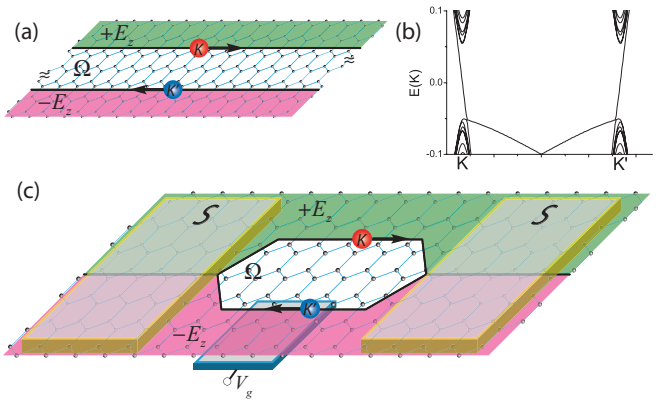

FIG. 1. (a) Schematic of two valley-chiral TISs between the $\pm E_z$ and Ω regions in a zigzag nanoribbon. Only the right-moving K valley (red ball) is conductive in the upper interface and the left-moving K' valley (blue ball) is permitted in the lower interface. (b) Low-energy band structure of the zigzag nanoribbon system. (c) A ring-shape Josephson junction based on the TISs of (a). Two yellow cuboids stand for the S banks and a blue cuboid for a voltage gate V_g applied to the lower interface.

[44] accounting for a quantum anomalous Hall state and can be realized by photoirradiation [35] with its strength Ω. $\langle ij\rangle$ denotes the nearest-neighboring sites, while $\langle\langle lm\rangle\rangle$ stands for the next-nearest-neighboring sites; $\mu_i = \pm 1$ for the i site representing the A or B atom (the honeycomb lattice possesses A and B inequivalent atoms); $\nu_{lm} = 1$ if the next-nearest-neighboring hopping is anticlockwise, while $\nu_{lm} = -1$ if it is clockwise with respect to the normal of the 2D sheet. The photoirradiation Ω is applied to the whole lattice in Fig. 1(a), while the static staggered potentials $\pm E_z$ are confined into one-third of the ribbon width and $|E_z| > |\Omega|$, which guarantees generation of TISs between different topological phases. Here no spin-related interaction is considered and the spin is degenerate.

The energy band of the nanoribbon lattice is presented in Fig. 1(b), and only two curves with a linear E-k dispersion (fulfilling the massless Dirac equation) reside in the bulk energy gap and cross the Fermi energy $E = 0$ at the K or K' points. They are exactly the two chiral TISs forming at the upper and lower interfaces displayed in Fig. 1(a), respectively. This comes from the fact that a TIS is generated when two neighboring insulators have different topological indices. The Ω term leads to a quantum anomalous Hall state [35,44], while the E_z term results in a quantum valley Hall insulator [34]. The two TISs come from different valleys and have opposite chiralities. Therefore, there is no direct coupling between them and thus no further excitation of TISs, as can seen from Fig. 1(b). In fact, these two TISs can be regarded as a single valley-helical *inner boundary* state connecting the neighboring insulating phases of E_z and $-E_z$, while the photoirradiation term [35] Ω introduced here makes them split in real space.

As is known, the two electrons of a singlet Cooper pair should stem, respectively, from the K and K' valleys ($K = -K'$) in the honeycomb-lattice system [45]. When the two separated TISs with opposite valley chiralities in Fig. 1(a) are integrated into a single ring-shape JJ like Fig. 1(c), a Cooper pair should span the two ring arms, the K and K' paths. A similar situation can occur in the JJ based on quantum Hall edge states due to a strong magnetic field [19]. Note that the sinuous path of TISs [Fig. 1(c)], and not a straight one [Fig. 1(a)], does not exert an influence on its topological properties.

In the following, we calculate the supercurrent sustained by TISs in the two-terminal lattice device [Fig. 1(c)]. The superconductivity in the left and right lattice leads is assumed from the superconducting proximity effect, which is described by $H_{l(r)} = \sum_{i\sigma} \Delta e^{i\varphi_{l(r)}} C^+_{i\sigma} C^+_{i\bar{\sigma}} + \text{c.c.}$, where $\bar{\sigma} = -\sigma$, $\varphi_{l(r)}$ is the left and right macroscopic superconducting phase, and Δ is the pair potential. The supercurrent is given by [46]

$$J = \frac{e}{\hbar}\int \frac{dE}{2\pi}\text{Tr}[G^<_{l,l+1}(E)\tilde{t}_{l+1,l} - \text{H.c.}], \tag{2}$$

where is $G^<(E)$ is the lesser Green's function, the subscript l is the index of the unit slice of the nanoribbon lattice, $\tilde{t}_{l+1,l}$ is the hopping matrix between the neighboring slices, and the trace is over the unit slice and electron space. At equilibrium, $G^< = [G^a - G^r]f(E)$, where $G^{r(a)}$ is the retarded (advanced) Green's function, and f is the Fermi-Dirac distribution function. It is emphasized that the thermal equilibrium case is considered here, and only these states below the Fermi energy contribute to the supercurrent at $T = 0$ K. For simplicity, a rectangle ring is adopted in concrete calculations and its width is one-third of the ribbon width N, its length is denoted by L, and the gate voltage V_g is symmetrically applied on the ring-shape TIS paths. This would not lead to the spatial phase oscillation of the induced superconductivity in honeycomb lattices [28], and so the constant order parameter considered in the two S leads is reasonable. The pair potential is set as $\Delta = 10^{-3}t$, where the hopping integral t is set as an energy unit $t = 1$. Since the mean-field BCS Hamiltonian is taken into account, the global Fermi energy of the system is taken as $E_F = 0.03t$, so that $E_F \gg \Delta$, and the superconducting length ξ_s is much longer than the Fermi wavelength λ_F, $\xi_s \gg \lambda_F$.

In Fig. 2(a), the supercurrent J versus $\varphi(= \varphi_r - \varphi_l)$ is plotted within different applied gate voltages V_g. It is seen that the JJ exhibits a clear anomalous Josephson effect, $J \sim \sin(\varphi + \varphi_0)$. The CPR curves deviate severely from the

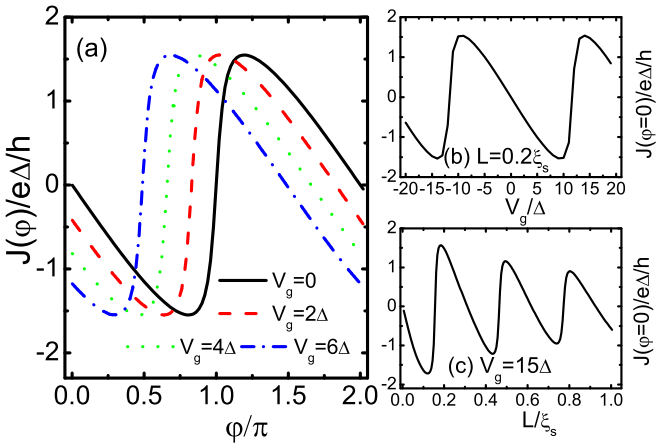

FIG. 2. Supercurrent (J) versus the phase difference φ (a), zero-phase supercurrent [$J(\varphi = 0)$] as a function of the gate voltage V_g (b), and the junction length L (c). Parameters are taken as $N = 96$, $E_z = 0.1t$, $\Omega = 0.05t$, $L = 0.2\xi_s$, $V_g = 15\Delta$.

sine function, because the junction itself is approximately transparent and the higher harmonic terms contribute to J non-negligibly. In Figs. 2(b) and 2(c), the zero-phase supercurrent $J(\varphi = 0)$ is presented as a function of V_g and the junction length L, and it exhibits similar oscillations. An increase of L results in a damped periodic oscillation, whereas V_g leads to a nondamped oscillation; the latter is related to the Dirac electron's property of TISs. This φ_0-JJ confirms the conjecture that the electron and hole quasiparticles will accumulate an effective dynamic phase difference due to V_g when they propagate along different paths, i.e., the superconducting phase shift could be $\varphi_0 \sim V_g L/\hbar v_F$ with the Fermi velocity v_F. Note no exchange field is considered here and the spin is by default degenerate in the device of Fig. 1(c).

To see the effective phase shift by V_g, we also calculate the Andreev bound states (ABS) in the superconducing energy gap, which are represented by the energy-resolved particle density distribution in Fig. 3. It is shown that when there is no voltage $V_g = 0$ in Fig. 3(a), the JJ exhibits a standard ABS of a topological JJ, i.e., even if there exists some pair breaking effect, $E(\varphi) < \Delta$, the Majorana zero-energy mode does not disappear and fixes at $\varphi = \pi$. The two counterpropagating valley-chiral TISs together in the device [Fig. 1(c)] originate from a valley-helical conductive channel, which fully resembles the spin-helical boundary state of a quantum spin Hall insulator [47]. Hence, the JJ here is also topological [48] by regarding the valley degree as the spin degree of electrons. When V_g is turned on, the zero-energy mode begins to deviate from $\varphi = \pi$ as shown in Figs. 3(b)–3(d), and the deviation is controlled by V_g as well as the junction length L. This indicates that a nonzero phase shift exists or the ground state of JJ deviates from $\varphi = 0$ as long as the two TISs have a static potential difference.

As can be seen from the ABS in Fig. 3, the suppression of the Cooper pair transport is obvious, $E(\varphi) < \Delta$, even at $L \ll \xi_s$. This mainly comes from the intervalley scattering due to the finite-size effect in the numerics. Since the valley degree of freedom is defined in the momentum space, any short-ranged disorder should lead to the intervalley scattering such as sharp edges of the nanoribbon lattice, E_z region, and S banks. Another factor for pair breaking is that the one-dimensional (1D) TIS has a finite-width distribution $\sim \hbar v_F/E_g$, where E_g is the smaller bulk energy gap of the two neighboring topological phases. It is emphasized that the 2π periodicity of the obtained supercurrent in Fig. 2 comes from the assumption of the junction being in the thermal equilibrium state [Eq. (2)], although the ABS above represents a typical topological Josephson junction.

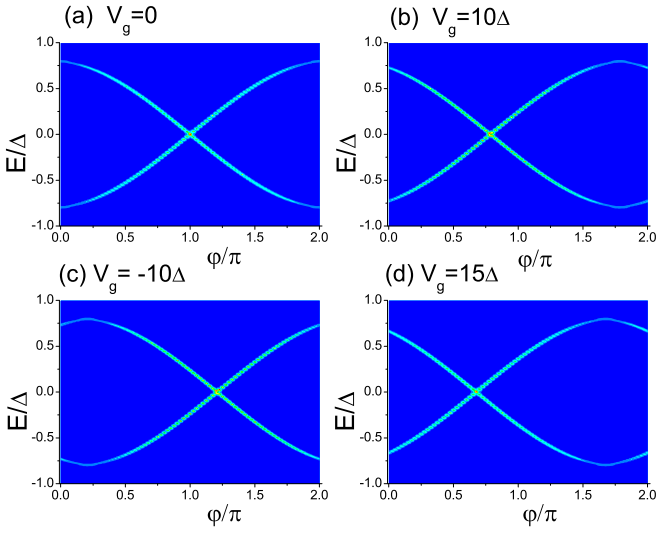

FIG. 3. Particle density distribution in the superconducting energy gap as a function of φ within an arbitrary unit. Parameters are taken as $N = 96$, $E_z = 0.1t$, $\Omega = 0.05t$, $L = 0.1\xi_s$, and the gate voltages are marked in each panel.

For the φ_0-JJ shown in Fig. 2, the key point is the quasiparticles in the nonsuperconducting link having a definite chirality, so the transport of quasiparticles is unidirectional, and the opposite $-\varphi_0$ phase shift to compensate is lacking. This can be understood from the ABS of an S/F/S junction [49], $E \sim \pm\Delta|\cos(\varphi/2 + \sigma h_e L/\hbar v_F)|$, with the exchange-field strength h_e and $\sigma = \pm 1$. Both spin-up and spin-down electrons can move in the same direction (nonchiral) and lead to an opposite phase shift. Therefore, one cannot obtain a φ_0 junction unless the F layer is a chiral metal [27] or has some additional spin-related interaction destroying the balance of spin-opposite phase shifts [15–17]. In the device of Fig. 1(c), the TISs are (valley) chiral and so, the φ_0-JJ arises.

III. π-JJ BASED ON VALLEY-HELICAL TIS

In the following, we will consider other two different cases to confirm the above extrapolation. The first model is the two TISs [Fig. 1(c)] changed to be valley helical not valley chiral, i.e., both K and K' valleys in each interface are moving oppositely, as shown in Fig. 4(a). The sum of these two TISs shall exhibit no valley chirality, and the φ_0-JJ should disappear. In order to keep the electron- and

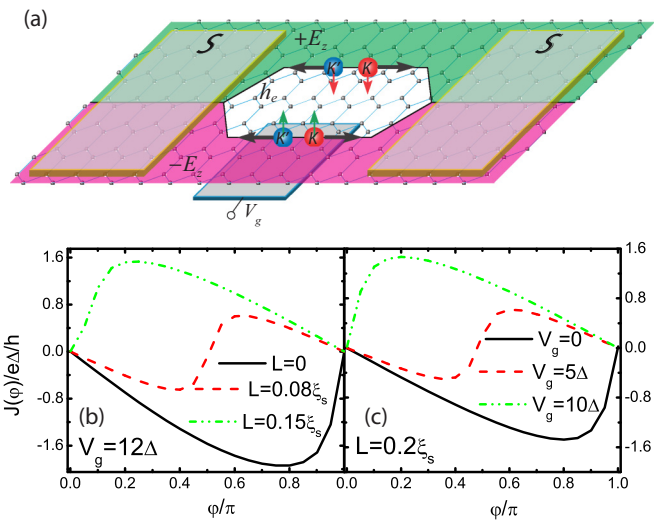

FIG. 4. (a) Setup of a valley-helical TIS-based Josephson junction. The staggered magnetization h_e substitutes the photoirradiation term Ω in [Fig. 1(c)] and others are the same. Each TIS permits the K and K' valley counterpropagating and is fully spin polarized. Spin-down electrons flow in the upper interface and spin-up electrons in the lower interface. The CPR is presented within different junction lengths L (b) and different voltages V_g (c). Parameters are $N = 96$, $E_z = 0.1t$, and $h_e = 0.05t$.

holelike quasiparticles separated spatially, we turn to employ the staggered magnetization [41,42] $\sum_{i\sigma}\mu_i h_e \sigma C^\dagger_{i\sigma}C_{i\sigma}$ to replace the photoirradiation term in Eq. (1), where h_e is the magnetization strength. The Hamiltonian is reexpressed as

$$\mathcal{H} = -t\sum_{\langle ij\rangle\sigma} C^\dagger_{i\sigma}C_{j\sigma} + \sum_{i\sigma}(\mu_i E_z + V_g)C^\dagger_{i\sigma}C_{i\sigma} + \sum_{i\sigma}\mu_i h_e \sigma C^\dagger_{i\sigma}C_{i\sigma}, \quad (3)$$

so each TIS will be fully spin polarized and valley helical. The band structure of this TIS can be found in Ref. [42].

Under the same parameters, the CPR $J(\varphi)$ is presented with a variation of the gate voltage V_g and the junction length L in Figs. 4(b) and 4(c). These curves exhibit typical 0-π state oscillations of the JJ, and there is no anomalous Josephson effect, no φ_0-JJ. The reason is the two TISs together [Fig. 4(a)] show no chirality of electrons; alternatively, both the K-valley and K'-valley quasiparticles accumulate an opposite dynamic phase $\pm\varphi_0$. This situation resembles a usual S/F/S junction, and a 0-π state oscillation appears.

IV. φ_0-JJ BASED ON SPIN-HELICAL EDGE STATES

Another model is to consider the S/F/S junction based on the spin-helical boundary state of a topological insulator [47], which is schematically shown in Fig. 5(a). Both the S and F banks cover only the lower edge states. For simplicity, the exchange-field ($\mathbf{h}_e$) direction is assumed along the spin eigendirection of boundary states, so it can shift spin bands but not open an energy gap [50]. The Kane-Mele topological insulator [51] is taken here, and in Eq. (1), the E_z term is replaced by a uniform magnetization $\mathbf{h}_e$ in the lower half of the ribbon, and Ω is replaced by $\lambda_{\rm soc}\sigma$, where $\lambda_{\rm soc}$ is the spin-orbit interaction strength. This S/F/S junction is thus described by the following Hamiltonian:

$$\mathcal{H} = -t\sum_{\langle ij\rangle\sigma} C^\dagger_{i\sigma}C_{j\sigma} + \sum_{i\sigma}(\sigma h_e)C^\dagger_{i\sigma}C_{i\sigma} + i\sum_{\langle\langle lm\sigma\rangle\rangle}\frac{\lambda_{\rm soc}\sigma\nu_{lm}}{3\sqrt{3}}C^\dagger_{l\sigma}C_{m\sigma}. \quad (4)$$

In numerics, $\lambda_{\rm soc} = 0.1t$ and other system parameters remain unchanged. The CPR is shown in Fig. 5(b) with different F exchange-field strengths h_e. It is seen that a nonzero supercurrent appears at zero phase $\varphi = 0$, and a φ_0-JJ state emerges. The zero-phase currents $J(\varphi = 0)$ in Figs. 5(c) and 5(d) show a damped oscillation with the junction length L and a nondamped oscillation with variation of h_e, which are the same as those in Figs. 2(b) and 2(c). This confirms that the electron chirality is vital for a φ_0-JJ, since in a usual (nonchiral) S/F/S junction, one can only obtain a π-state JJ by controlling h_e or L. It is evident that when the F direction rotates, the

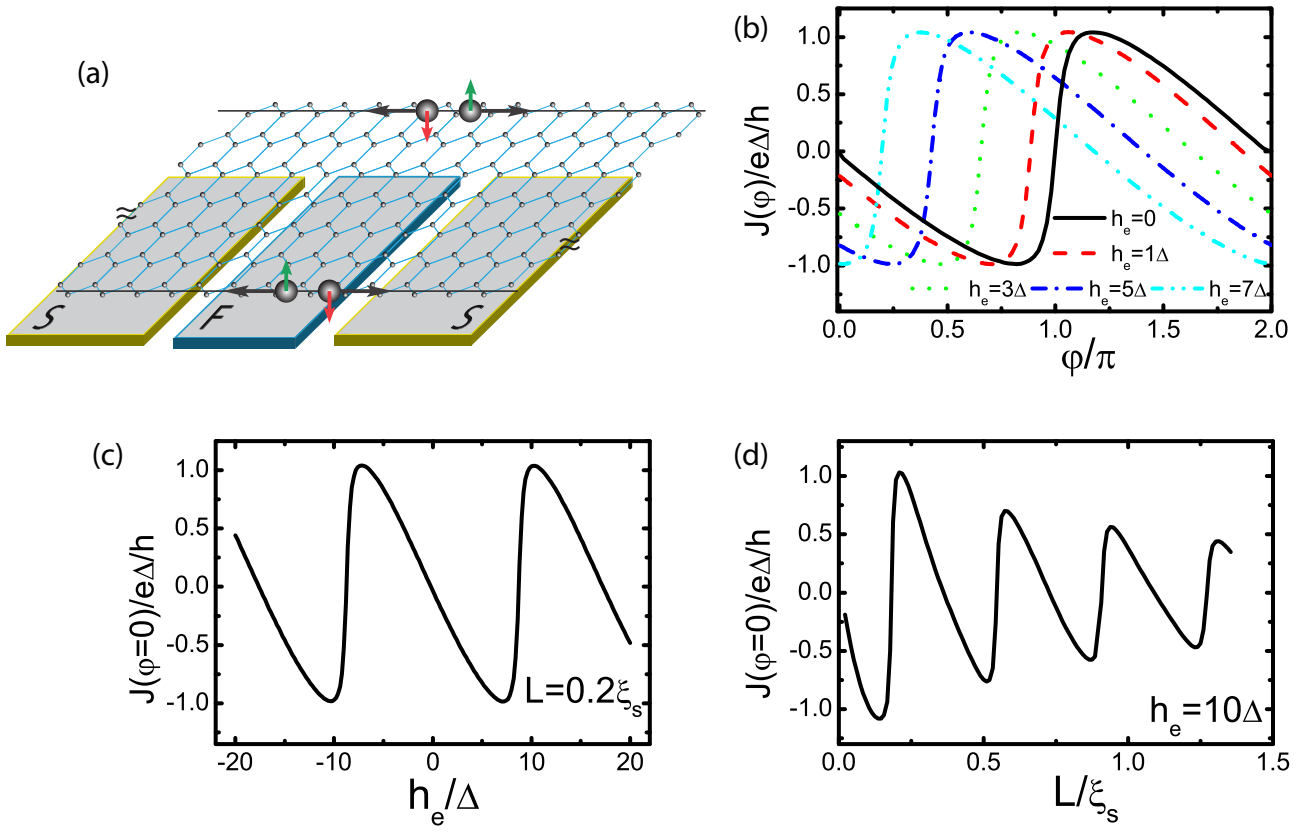

FIG. 5. (a) Schematic of an S/F/S junction based on the helical boundary states of a quantum spin Hall insulator. The S and F are deposited on the lower edge of the topological insulator and two opposite spins are counterpropagating in each edge. (b) Current-phase relation $J(\varphi)$ versus different exchange-field strengths h_e. Zero-phase supercurrent $J(\varphi = 0)$ as a function of h_e (c) and the junction length L (d). Parameters are $N = 96$, $\lambda_{\rm soc} = 0.1t$, $L = 0.2\xi_s$, $h_e = 10\Delta$.

φ_0 should be changed correspondingly [27]. Furthermore, the helical boundary state shall be separated in real space [50] like the split valley-helical TIS in Fig. 1(c). This also makes electric control of the phase shift φ_0 feasible.

V. CONTINUUM MODEL FOR ABS

Since the studied JJ [Fig. 1(c)] is actually based on the linear Dirac electron's behavior of the TISs, one can use a simplified 1D wire to model this JJ, which is given by

$$H_s = (-i\hbar v_F \partial/\partial_x + U(x))\varsigma_z\eta_z - \mu\varsigma_z + \Delta(x)(\cos\varphi_x\varsigma_x + \sin\varphi_x\varsigma_y), \quad (5)$$

where $\varsigma_{x,y,z}$ is the Pauli operator representing the e-h space, η_z is the valley Pauli operator, μ is the chemical potential, and $\Delta(x) = \Delta[\theta(x - L/2) + \theta(x + L/2)]$ is limited in left ($x < -L/2$) and right ($x > L/2$) S banks, $\varphi_x = \varphi_{l(r)}$ for $x < -L/2$ ($x > L/2$), $\theta(x)$ is a step function, the potential $U(x) = V_g\theta(L/2 - x)\theta(x + L/2)$ is considered in the middle nonsuperconducting region, and V_g makes a potential difference only between the K and K' valley channels without opening an energy gap of Dirac electrons. However, it breaks the time-reversal symmetry in the above Hamiltonian. The spin degree of freedom is neglected while the valley-helicity is considered in this 1D model.

The ABS can be directly derived out as

$$\arccos(E/\Delta) = (\eta V_g + E)L/\hbar v_F + \varphi/2. \quad (6)$$

When $L \ll \xi_s$, one can obtain $E = \pm\Delta|\cos(\varphi/2 + \eta\gamma/2)|$, $\gamma = 2V_gL/\hbar v_F$, $\eta = \pm 1$ depending on the K-valley chirality, i.e., the K-valley electrons move forward ($\eta = 1$) or backward ($\eta = -1$) along the x axis. It is seen that the gate voltage V_g merely shifts the superconducting phase φ by γ but has no influence on the junction transparency. The reason is the linear energy dispersion of Dirac electrons of TISs. As long as the intervalley scattering exists, the junction is not transparent since it can open an energy gap of the TISs, where the ABS is given by [52] $E = \pm\sqrt{T_0}\Delta|\cos(\varphi/2 + \eta\gamma/2)|$, with T_0 the interface transmission of the junction. This formula coincides with numerical ABSs shown in Fig. 3. The phase shift γ here also approximates the numerical one, e.g., γ is estimated to be 0.31π with those parameters used in Fig. 3(b), where the numerical phase shift is about 0.24π. Therefore, it is the electron chirality and V_g (breaking the time-reversal symmetry) together that lead to an electrically controllable φ_0-JJ shown in Figs. 3 and 2.

Finally, it is worth pointing out that an extra interaction breaking the time-reversal symmetry must be introduced to split the topologically protected helical interface or boundary state in real space so that a static potential can make a difference on the CPR. Besides the buckled silicene, stanene, or germanene [36–40] that can be used to realize our proposal, the bilayer graphene is also a good candidate material, because the TIS constructed by the interlayer potentials was already displayed in experiment [53], and Cooper-pair splitting in real space was also shown theoretically based on the valley-dependent TIS [43].

VI. CONCLUSION

In summary, we have found an electrically controllable φ_0 Josephson junction based on a valley-helical state in 2D buckled honeycomb-lattice systems. It was shown that when the valley-helical state is separated into two opposite chiral states in real space by photoirradiation, a static potential difference between them could control the phase shift φ_0 of this anomalous Josephson effect. Our findings shall shed light on producing arbitrary superconducting phase batteries.

ACKNOWLEDGMENT

The work described in this paper is supported by the NSFC (Grants No. 11274059, No. 115074045, and No. 11204187) and the NSF of Jiangsu Province (Grant No. BK20131284).

[1] A. A. Golubov, M. Yu. Kupriyanov, and E. Il'ichev, Rev. Mod. Phys. **76**, 411 (2004).
[2] L. B. Ioffe, V. B. Geshkenbein, M. V. Feigel'man, A. L. Fauchere, and G. Blatter, Nature (London) **398**, 679 (1999).
[3] G. Blatter, V. B. Geshkenbein, and L. B. Ioffe, Phys. Rev. B **63**, 174511 (2001).
[4] A. V. Ustinov and V. K. Kaplunenko, J. Appl. Phys. **94**, 5405 (2003).
[5] T. Yamashita, K. Tanikawa, S. Takahashi, and S. Maekawa, Phys. Rev. Lett. **95**, 097001 (2005).
[6] A. K. Feofanov, V. A. Oboznov, V. V. Bol'ginov, J. Lisenfeld, S. Poletto, V. V. Ryazanov, A. N. Rossolenko, M. Khabipov, D. Balashov, A. B. Zorin, P. N. Dmitriev, V. P. Koshelets, and A. V. Ustinov, Nat. Phys. **6**, 593 (2010).
[7] V. V. Ryazanov, V. A. Oboznov, A. Y. Rusanov, A. V. Veretennikov, A. A. Golubov, and J. Aarts, Phys. Rev. Lett. **86**, 2427 (2001).
[8] T. Kontos, M. Aprili, J. Lesueur, F. Genet, B. Stephanidis, and R. Boursier, Phys. Rev. Lett. **89**, 137007 (2002).
[9] A. I. Buzdin, Rev. Mod. Phys. **77**, 935 (2005).
[10] F. S. Bergeret, A. Volkov, and K. Efetov, Rev. Mod. Phys. **77**, 1321 (2005).
[11] I. V. Krive, A. M. Kadigrobov, R. I. Shekhter, and M. Jonson, Phys. Rev. B **71**, 214516 (2005).
[12] A. A. Reynoso, G. Usaj, C. A. Balseiro, D. Feinberg, and M. Avignon, Phys. Rev. Lett. **101**, 107001 (2008).
[13] A. Buzdin, Phys. Rev. Lett. **101**, 107005 (2008).
[14] A. Zazunov, R. Egger, T. Jonckheere, and T. Martin, Phys. Rev. Lett. **103**, 147004 (2009).
[15] Jun-Feng Liu and K. S. Chan, Phys. Rev. B **82**, 125305 (2010).
[16] Jun-Feng Liu and K. S. Chan, Phys. Rev. B **82**, 184533 (2010).
[17] Jun-Feng Liu, K. S. Chan, and J. Wang, J. Phys. Soc. Jpn. **80**, 124708 (2011).
[18] F. Dolcini and F. Giazotto, Phys. Rev. B **75**, 140511(R) (2007).
[19] J. A. M. van Ostaay, A. R. Akhmerov, and C. W. J. Beenakker, Phys. Rev. B **83**, 195441 (2011); M. Stone and Y. Lin, *ibid.* **83**, 224501 (2011).
[20] A. Buzdin and A. E. Koshelev, Phys. Rev. B **67**, 220504(R) (2003).

[21] A. Gumann and N. Schopohl, Phys. Rev. B **79**, 144505 (2009).
[22] N. G. Pugach, E. Goldobin, R. Kleiner, and D. Koelle, Phys. Rev. B **81**, 104513 (2010).
[23] E. Goldobin, D. Koelle, R. Kleiner, and R. G. Mints, Phys. Rev. Lett. **107**, 227001 (2011).
[24] H. Sickinger, A. Lipman, M. Weides, R. G. Mints, H. Kohlstedt, D. Koelle, R. Kleiner, and E. Goldobin, Phys. Rev. Lett. **109**, 107002 (2012).
[25] E. Goldobin, H. Sickinger, M. Weides, N. Ruppelt, H. Kohlstedt, R. Kleiner, and D. Koelle, Appl. Phys. Lett. **102**, 242602 (2013).
[26] A. Lipman, R. G. Mints, R. Kleiner, D. Koelle, and E. Goldobin, Phys. Rev. B **90**, 184502 (2014).
[27] Y. Tanaka, T. Yokoyama, and N. Nagaosa, Phys. Rev. Lett. **103**, 107002 (2009); A. M. Black-Schaffer and J. Linder, Phys. Rev. B **83**, 220511(R) (2011).
[28] F. Dolcini, M. Houzet, and J. S. Meyer, Phys. Rev. B **92**, 035428 (2015).
[29] M. Ezawa, New J. Phys. **14**, 033003 (2012).
[30] M. Ezawa, Phys. Rev. B **88**, 161406(R) (2013).
[31] H. Pan, X. Li, F. Zhang, and S. A. Yang, Phys. Rev. B **92**, 041404(R) (2015).
[32] S. K. Wang, J. Wang, and K. S. Chan, New J. Phys. **16**, 045015 (2014).
[33] D. S. L. Abergel, J. M. Edge, and A. V. Balatsky, New J. Phys. **16**, 065012 (2014).
[34] D. Xiao, W. Yao, and Q. Niu, Phys. Rev. Lett. **99**, 236809 (2007).
[35] M. Ezawa, Phys. Rev. Lett. **110**, 026603 (2013).
[36] P. Vogt, P. De Padova, C. Quaresima, J. Avila, E. Frantzeskakis, M. C. Asensio, A. Resta, B. Ealet, and G. Le Lay, Phys. Rev. Lett. **108**, 155501 (2012).
[37] S. Cahangirov, M. Topsakal, E. Akturk, H. Sahin, and S. Ciraci, Phys. Rev. Lett. **102**, 236804 (2009).
[38] S. Lebegue and O. Eriksson, Phys. Rev. B **79**, 115409 (2009).
[39] C.-C. Liu, W. Feng, and Y. Yao, Phys. Rev. Lett. **107**, 076802 (2011).
[40] Y. Xu, B. Yan, H.-J. Zhang, J. Wang, G. Xu, P. Tang, W. Duan, and S.-C. Zhang, Phys. Rev. Lett. **111**, 136804 (2013).
[41] X. Li, T. Cao, Q. Niu, J. Shi, and J. Feng, Proc. Natl. Acad. Sci. USA **110**, 3738 (2013).
[42] J. Wang, L. Hao, and K. S. Chan, Phys. Rev. B **91**, 085415 (2015).
[43] A. Schroer, P. G. Silvestrov, and P. Recher, Phys. Rev. B **92**, 241404(R) (2015).
[44] F. D. M. Haldane, Phys. Rev. Lett. **61**, 2015 (1988).
[45] C. W. J. Beenakker, Phys. Rev. Lett. **97**, 067007 (2006); A. R. Akhmerov and C. W. J. Beenakker, *ibid.* **98**, 157003 (2007).
[46] J. Wang, Y. H. Yang, and K. S. Chan, Phys. Rev. B **89**, 064501 (2014).
[47] X.-L. Qi and S.-C. Zhang, Rev. Mod. Phys. **83**, 1057 (2011).
[48] M. Ezawa, Phys. Rev. Lett. **114**, 056403 (2015).
[49] J. Cayssol and G. Montambaux, Phys. Rev. B **70**, 224520 (2004).
[50] H. Li, L. Sheng, R. Shen, L. B. Shao, B. Wang, D. N. Sheng, and D. Y. Xing, Phys. Rev. Lett. **110**, 266802 (2013).
[51] C. L. Kane and E. J. Mele, Phys. Rev. Lett. **95**, 226801 (2005).
[52] Z. H. Yang, J. Wang, and K. S. Chan, J. Phys.: Condens. Matter **23**, 085701 (2011).
[53] L. Ju, Z. Shi, N. Nair, Y. Lv, C. Jin, J. Velasco Jr., C. Ojeda-Aristizabal, H. A. Bechtel, M. C. Martin, A. Zettl, J. Analytis, and F. Wang, Nature **520**, 650 (2015).